Acta Crystallographica Section F
Structural Biology and Crystallization Communications
ISSN 1744-3091

Crystallization and preliminary crystallographic study of a trypsin-resistant catalytic domain of human calcineurin

Lei Jin,[a] Michael H. A. Roehrl,[b] Li Xiao,[a] Xiuyun He,[a] Haibin Li,[a] Linhu Ge[a] and Bingyi Shi[a]*

[a]Organ Transplant Center, Beijing 309 Hospital, 17A Hei-shan-hu Road, Haidian District, Beijing 100091, People's Republic of China, and [b]Department of Pathology and Laboratory Medicine, School of Medicine, Boston University, 670 Albany Street, Boston, MA 02118, USA

Correspondence e-mail: shibingyi@medmail.com.cn

Received 18 November 2011
Accepted 22 February 2012

Calcineurin, a Ca^{2+}/calmodulin-dependent serine/threonine protein phosphatase, plays a key role in a number of cellular pathways, including T-cell activation, and is an important molecular target of the immunosuppressive drugs cyclosporin A and FK506. To understand the structural basis underlying the activation of calcineurin by calmodulin, X-ray crystallography was employed to solve the three-dimensional structure of the free calcineurin catalytic domain (residues 20–347 of the A subunit). To accomplish this, a bacterially expressed glutathione *S*-transferase (GST) fusion protein of the human calcineurin catalytic domain was first purified by GST-affinity chromatography. After limited digestion by trypsin, the catalytic domain (Cncat) was purified using anion-exchange and size-exclusion chromatography. Crystallization of Cncat was achieved by the hanging-drop vapour-diffusion method at pH 6.5 using PEG 6000 as precipitant. The diffraction results showed that the Cncat crystal belonged to the orthorhombic space group $P2_12_12$, with unit-cell parameters a = 161.6, b = 87.4, c = 112.0 Å. There are four Cncat molecules in the asymmetric unit, with 49.5% solvent content. An X-ray diffraction data set was collected to 2.87 Å resolution and a clear molecular-replacement solution was obtained. The active site of Cncat is open to the solvent channels in the crystal packing.

1. Introduction

Calcineurin (Cn; also known as protein phosphatase 3, and formerly as protein phosphatase 2B) is a Ca^{2+}/calmodulin-dependent serine/threonine protein phosphatase. It participates in a number of cellular regulatory pathways, including the activation and nuclear translocation of the transcriptional regulator nuclear factor of activated T cells (NFAT; Klee *et al.*, 1979; Aramburu *et al.*, 2000; Clipstone & Crabtree, 1992). Cn is an important molecular target of the immunosuppressive drugs cyclosporin A and FK506 (Liu *et al.*, 1991; O'Keefe *et al.*, 1992). Cn is heterodimeric and has two subunits: a catalytic A subunit (CnA) and a Ca^{2+}-binding regulatory B subunit (CnB). CnA comprises four regions: a catalytic domain (residues 20–340), a CnB-binding segment (residues 349–372), a calmodulin-binding segment (residues 390–414) and a C-terminal auto-inhibitory helix (residues 469–486). CnB bears four Ca^{2+} ions and binds to an extended five-turn α-helix of CnA. The CnB-binding segment of CnA then projects away from the body of the catalytic domain; binding of CnB renders this helix stable in its projecting conformation. Calmodulin binds the segment between the CnB site and the auto-inhibitory helix of CnA (Kissinger *et al.*, 1995) (Fig. 1*a*). Four types of Cn crystal structures have been reported in the literature: self-inhibited full-length Cn (Kissinger *et al.*, 1995), FK506/FKBP-inhibited Cn (Griffith *et al.*, 1995; Kissinger *et al.*, 1995), cyclosporin/cyclophilin-inhibited Cn (Jin & Harrison, 2002; Huai *et al.*, 2002) and NFAT peptide-bound truncated Cn with an intact B subunit (Li *et al.*, 2007). Owing to the lack of the structure of the Cn–calmodulin complex, it is still not well understood how the binding of calmodulin activates Cn. It is hypothesized that calmodulin binding can stiffen the segment consisting of residues 390–414 into an

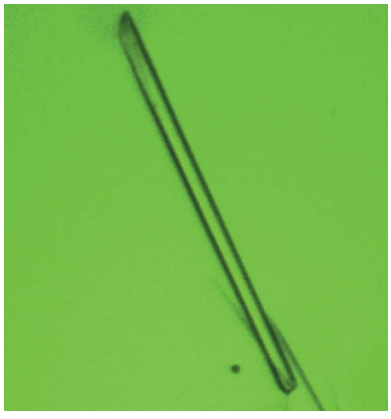

α-helical conformation and thereby pull the auto-inhibitory helix away from the catalytic site, leading to Cn activation. To better understand the structural basis underlying Cn activation by calmodulin, we set out to use X-ray crystallography to solve the three-dimensional structure of the free and active Cn catalytic domain. We hope that it will help to answer some of the fundamental questions regarding activation of Cn. For example, comparing the structure of the auto-inhibited full-length Cn with that of the free catalytic domain will provide a definite answer as to whether the active site of Cn itself exists in a pre-formed active conformation.

Deciphering the structure of the active site of Cn in its active state also has significant medical implications for the discovery and development of new Cn inhibitors. Cyclosporin and FK506 are Cn inhibitors and have long been used clinically to prevent graft rejection after organ transplantation and to treat autoimmune diseases. After entering the cell, the two drugs first form a binary complex with their cellular receptors (cyclophilin and FK506-binding proteins, respectively). The binary complexes do not inhibit calcineurin by directly contacting the active site, but instead bind to a nearby site, thus physically blocking the accessibility of the active site to its physiological protein substrates (Kissinger *et al.*, 1995; Griffith *et al.*, 1995; Jin & Harrison, 2002; Huai *et al.*, 2002). Serious side effects have been associated with the use of these two drugs, *e.g.* chronic nephrotoxicity, post-transplantation diabetes mellitus and hypertension (Bai *et al.*, 2010; Halloran, 2004). A recent finding indicated that FK506 itself can cause hypertension by activating the renal sodium chloride cotransporter (Hoorn *et al.*, 2011). Therefore, direct and specific small-molecule inhibitors targeting the active site of Cn may be an attractive alternative to cyclosporin and FK506. Several such inhibitors have already been described (Baba *et al.*, 2003, 2005). For the discovery and structure-based drug development of specific small-molecule inhibitors targeting the active site of Cn, we have also been searching for a Cn crystal form that would permit complex formation by ligand-soaking (Nienaber *et al.*, 2000) or cocrystallization techniques.

Here, we report the crystallization of a trypsin-resistant catalytic domain of human calcineurin α (A subunit, residues 20–347). A preliminary crystallographic study of the X-ray diffraction data is also presented. We have solved the structure by molecular replacement. Analysis of crystal packing revealed that the Cn active site is open to the solvent channels, which is ideal for inhibitor soaking and/or cocrystallization.

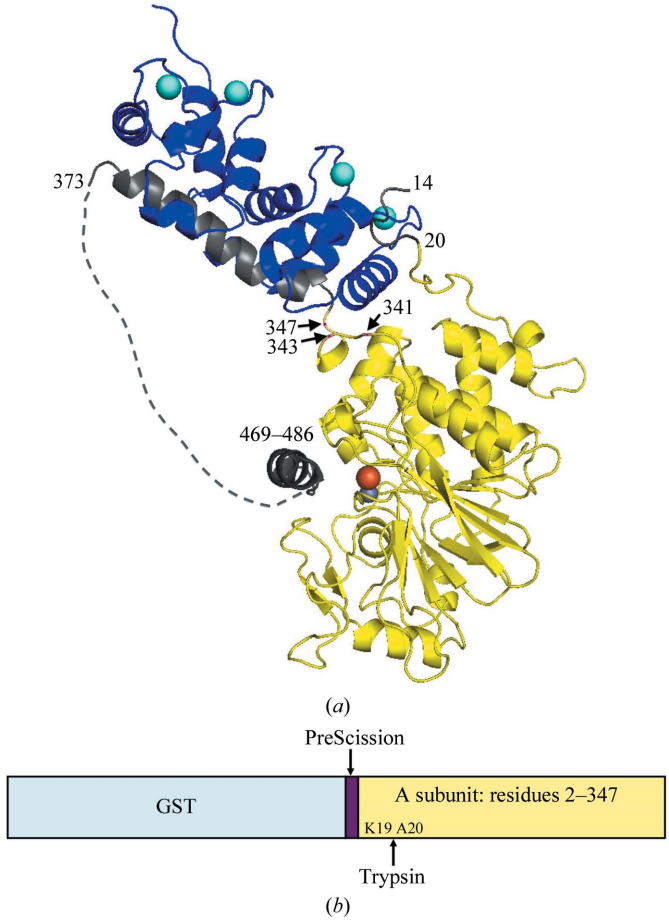

Figure 1
(*a*) Ribbon diagram of the crystal structure of auto-inhibited full-length human calcineurin, illustrating its heterodimeric organization. CnA is shown in yellow (residues 20–347) and grey. CnA has a dimetal centre at its active site containing Zn^{2+} (light blue) and Fe^{3+} (orange). The dashed line represents the calmodulin-binding segment, which was not observed in the crystal structure. CnB (blue) binds four calcium ions (cyan). Residue numbers are for CnA. The positions of residues Tyr341, Leu343 and Met347 are indicated by arrows. (*b*) Schematic drawing illustrating the design of the GST-fusion protein and the Cncat fragment which includes residues 20–347 as a result of trypsin cleavage of the fusion protein.

2. Materials and methods

2.1. Expression, purification and phosphatase activity of Cncat

The catalytic domain (Cncat) of human calcineurin α (NCBI accession No. NP_000935) comprises residues 20–347 of the A chain with Y341S, L343A and M347D substitutions to increase the local hydrophilicity for improved protein solubility. These residues are located on a turn connecting the main catalytic domain to the CnB-binding helix and are >20 Å away from the active site. Therefore, their mutation will presumably not affect the enzymatic activity of Cncat (Fig. 1*a* and Supplementary Fig. S1[1]). Cncat was produced as a GST-fusion protein. The bacterial expression plasmid for the GST-Cncat fusion protein was constructed in pGEX6P-1 vector (Amersham Pharmacia Biosciences) with a PreScission protease cleavage site C-terminal to the GST moiety (Fig. 1*b*; Aramburu *et al.*, 1999). Transformed *Escherichia coli* BL21 cells were cultured in LB medium and induced with isopropyl β-D-1-thiogalactopyranoside (IPTG). GST-Cncat fusion protein was purified by glutathione-Sepharose affinity chromatography. Cncat was then released by limited trypsin proteolysis of the fusion protein and was further purified by anion-exchange and size-exclusion chromatography.

The phosphatase activity of Cncat was determined using the Calbiochem calcineurin assay kit (EMD Biosciences, USA) with the RII phosphopeptide as the substrate at 0.15 m*M* final concentration according to the manufacturer's manual. 25 µl 2× buffer, 10 µl dH_2O and 10 µl RII phosphopeptide were mixed with 5 µl Cncat at varying concentrations on a microtitre plate provided in the assay kit. The amount of Cncat in the reaction was in the range of 0.14–0.37 µg. After the mixture had been incubated at 303 K for 30 min, 100 µl Malachite Green was added to terminate the reaction and to detect the released free phosphate. All reactions were performed in triplicate. After 30 min of colour development, the absorbance at 620 nm was measured on a microplate reader. A phosphate standard curve was also prepared according to the manufacturer's manual.

[1] Supplementary material has been deposited in the IUCr electronic archive (Reference: UO5034).

2.2. Crystallization

Cncat was concentrated to 5.0 mg ml^{-1} in 10 m*M* Tris–HCl pH 7.4, 50 m*M* NaCl, 1 m*M* $CaCl_2$ using an Amicon centrifugal filter with a 10 kDa molecular-weight cutoff (Millipore, USA). Preliminary crystallization conditions were screened with the Crystal Screen kits from Hampton Research (Aliso Viejo, California, USA) using the hanging-drop vapour-diffusion method. Hanging drops consisting of 1 µl protein solution and 1 µl crystallization solution were equilibrated against a reservoir containing 1 ml crystallization solution.

After optimization of initial crystallization conditions, 4 µl protein solution and 4 µl crystallization solution were mixed in a hanging drop, equilibrated against 1 ml crystallization solution and kept at 294 K in order to obtain crystals with larger dimensions.

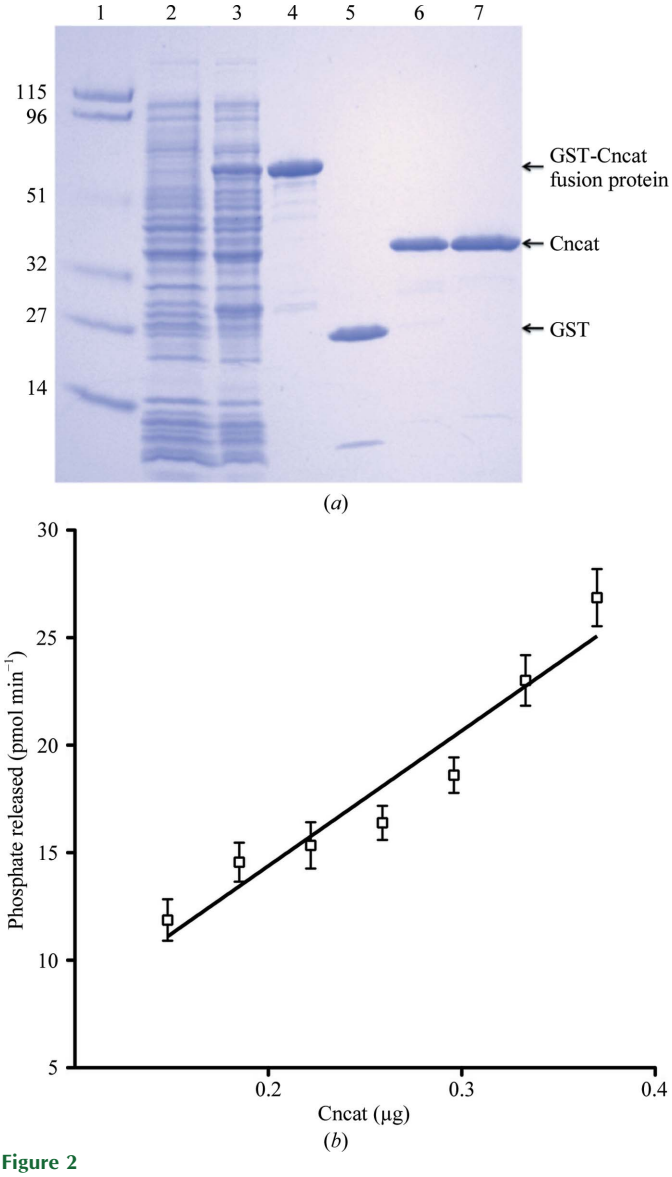

Figure 2
(*a*) SDS–PAGE of Cncat at different purification stages on a 4–20% gel under reducing conditions. Lane 1, molecular-weight markers (kDa). Lane 2, non-induced cells. Lane 3, IPTG-induced cells, showing an induced band for the fusion protein when compared with lane 2. Lane 4, GST-fusion protein eluted from glutathione-Sepharose. Lane 5, GST re-absorbed on glutathione-Sepharose beads after trypsin digestion. There is no fusion protein left, indicating complete trypsin digestion. Lane 6, Cncat released from the glutathione-Sepharose into the supernatant after trypsin digestion. Lane 7, final Cncat sample after Q-Sepharose and S-200 SEC purification. (*b*) Phosphatase activity of Cncat as determined by the RII dephosphorylation assay. Data points are means ± SEM of triplicates. The linear regression has $R^2 = 0.9024$ and $p < 0.0001$.

2.3. Data collection and processing

The Cncat crystal was cryoprotected using reservoir solution supplemented with 20%(*v*/*v*) glycerol and flash-cooled in liquid nitrogen. X-ray diffraction data were collected at 100 K on beamline X25 at the National Synchrotron Light Source, Brookhaven National Laboratory. Diffraction patterns were recorded on a CCD detector with a crystal-to-detector distance of 249.3 mm. The oscillation angle was 0.5° and the exposure time was 30 s per frame. A total of 300 frames were collected. Diffraction data were processed using the *HKL*-2000 suite (Otwinowski & Minor, 1997).

2.4. Phasing by molecular replacement

The *CNS* program (Brünger *et al.*, 1998) was used to solve the crystal structure of Cncat by molecular replacement. The starting model was obtained from the 2.1 Å resolution crystal structure of full-length human Cn (PDB entry 1aui; residues 27–340 of the A chain; Kissinger *et al.*, 1995). The cross-rotation function and translation function were calculated using data in the resolution range 15.0–4.0 Å. The top 15 peaks in the cross-rotation searches were used in the subsequent translation search. Rigid-body refinement (using the four molecules in the asymmetric unit as independent segments) was performed to improve the molecular-replacement solution and was followed by simulated annealing using *CNS*. Electron-density maps (both $2F_o - F_c$ and $F_o - F_c$ difference maps) were calculated with σ_A-weighting and bulk-solvent correction using *CNS*. Protein models and electron-density maps were visualized using *O* (Jones *et al.*, 1991). Molecular figures were prepared using *PyMOL* (DeLano, 2002).

3. Results and discussion

3.1. Cncat expression, purification and activity measurements

Transformed *E. coli* strain BL21 cells (Stratagene) were grown at 310 K in LB medium. After reaching an OD_{600} of 0.6, GST-Cncat expression was induced by addition of 1 m*M* IPTG. 6 l of cells were harvested after 5 h induction. The harvested cells were resuspended in PBS and protease-inhibitor cocktail (Roche, USA) at 277 K. The

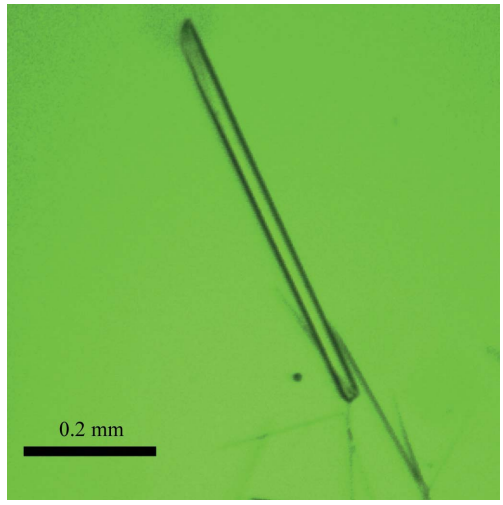

Figure 3
Picture of the Cncat crystals.

suspended cells were then disrupted by sonication and the insoluble fraction was removed by centrifugation for 20 min at 15 000*g*. The supernatant was applied onto a 10 ml column of Glutathione-Sepharose 4 Fast Flow. After extensively washing the resin with 50 m*M* Tris–HCl pH 7.4, 250 m*M* NaCl, GST-Cncat was eluted with 50 ml PBS, 10 m*M* reduced glutathione. The eluted GST-Cncat (Fig. 2, lane 4) was buffer-exchanged to 10 m*M* Tris–HCl pH 7.4, 100 m*M* NaCl, 1 m*M* $CaCl_2$ by ultrafiltration. 1 mg TPCK-treated trypsin (dissolved in 1 m*M* HCl) was added for limited proteolysis and the solution was left on ice for 4 h. The solution was then passed through a 0.5 ml benzamidine-Sepharose column and a 5 ml glutathione-Sepharose column sequentially to remove trypsin and GST (Fig. 2, lane 5). Cncat in the elution was further purified using Q Sepharose and Superdex 200 columns (Amersham Pharmacia Biosciences). The final buffer conditions for the Superdex 200 column were 10 m*M* Tris–HCl pH 7.4, 50 m*M* NaCl, 1 m*M* $CaCl_2$ (Sigma–Aldrich, USA). Cncat production and purification was monitored by reducing SDS–PAGE using 4–20% gradient gels (Life Technologies, USA; Fig. 2*a*). N-terminal sequencing indicated that trypsin cleavage occurred between Lys19 and Ala20, generating Cncat (residues 20–347). The quality and structural integrity of Cncat were good as assessed by matrix-assisted laser desorption ionization/time-of-flight (MALDI–TOF) mass spectrometry and NMR spectroscopy (Roehrl *et al.*, 2004).

Cncat was enzymatically active in the RII phosphopeptide dephosphorylation assay. Its specific activity was determined to be 64.70 pmol min^{-1} μg^{-1} under the conditions described in §2 (Fig. 2*b*).

3.2. Crystallization

Initial Cncat crystals were obtained using crystal screening kits from Hampton Research. Crystals were found in conditions with PEG as a precipitant. Further optimization of the crystal-growth conditions, including the pH, protein concentration and precipitant concentration, resulted in crystals of diffraction quality (Fig. 3). Crystals grew in 200 m*M* sodium acetate pH 6.5, 14%(*w*/*v*) PEG 6000 at 294 K. Crystals appeared within 24 h as thin rods and grew to maximum dimensions of ~0.6 × 0.02 × 0.02 mm in 10 d.

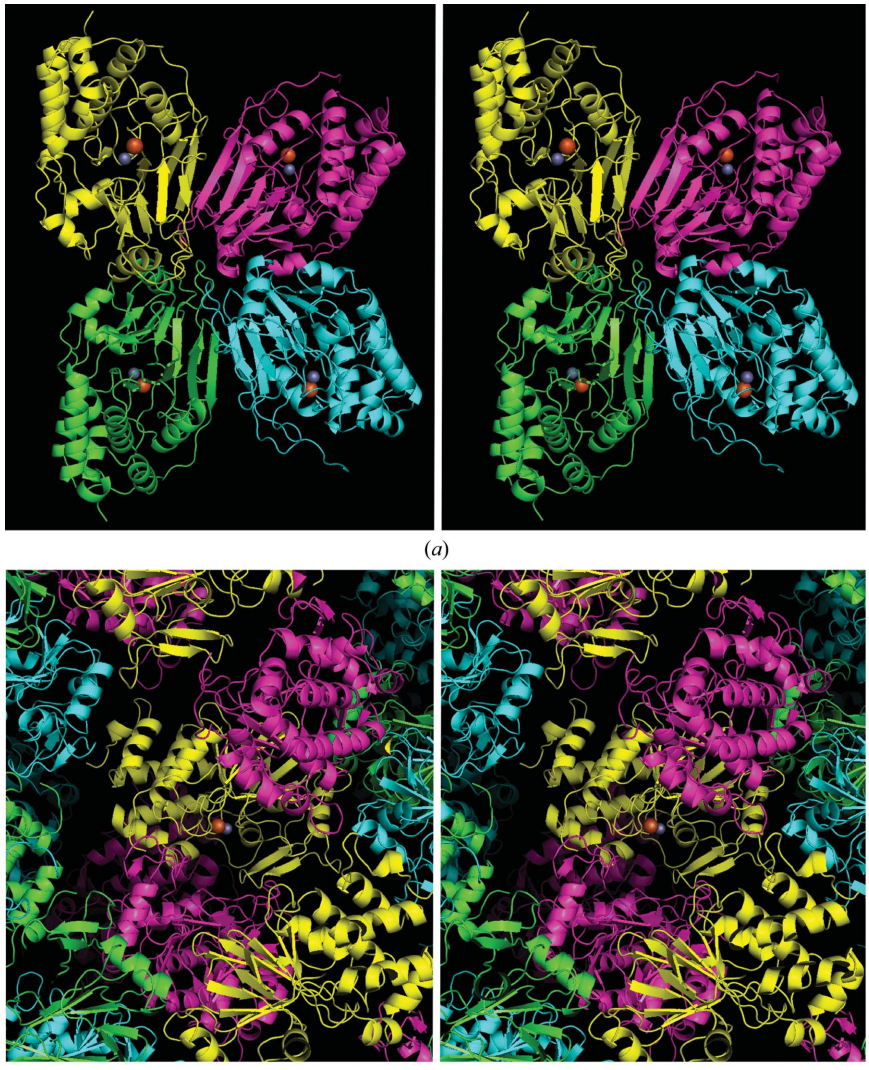

(*a*)

(*b*)

Figure 4
(*a*) Stereoview of the four Cncat molecules (yellow, magenta, cyan and green) in the asymmetric unit. The dimetal centres at the active sites are shown as light blue (Zn^{2+}) and orange (Fe^{3+}) spheres. (*b*) Stereoview of the Cncat active site (indicated by the dimetal centre) open to solvent channels. Only the open access for the central yellow Cncat is shown. The other active sites of Cncat are also open to the solvent channels in the crystal packing.

Table 1
X-ray data-collection statistics.

Values in parentheses are for the highest resolution shell.

Wavelength (Å)	1.100
Resolution range (Å)	20.0–2.87 (2.94–2.87)
Space group	$P2_12_12$
Unit-cell parameters (Å)	a = 161.6, b = 87.4, c = 112.0
No. of observed reflections	145819 (8762)
No. of unique reflections	36862 (2306)
Multiplicity	3.9 (3.8)
Completeness (%)	97.9 (87.0)
$R_{\rm merge}$† (%)	8.5 (23.2)
$\langle I/\sigma(I)\rangle$	14.0 (6.4)

† $R_{\rm merge} = \sum_{hkl}\sum_i |I_i(hkl) - \langle I(hkl)\rangle| / \sum_{hkl}\sum_i I_i(hkl)$, where $I_i(hkl)$ is the ith observation of reflection hkl and $\langle I(hkl)\rangle$ is the weighted average intensity for all observations i of reflection hkl.

3.3. X-ray data collection and processing

For cryoprotection, the crystal was briefly (about 8 s) soaked in reservoir solution supplemented with 20%(*v*/*v*) glycerol and flash-cooled in liquid nitrogen. We found that longer soaking in the cryoprotection solution significantly increased the mosaicity of the crystal. The Cncat crystals diffracted to a resolution beyond 2.8 Å using synchrotron radiation as an X-ray source. The crystal used for data collection was relatively thin, forcing us to use a 30 s exposure for each frame. Anisotropy was visually checked and was not significantly evident for reflections at lower than 2.8 Å resolution. We collected a large angular range (150° in total) of data as shown by the data multiplicity. Crystal decay was evident to some degree for the reflections beyond 2.8 Å, but was quite moderate for lower resolution shells. We therefore collected and processed the data to 2.87 Å resolution using *HKL*-2000, which gave an overall mosaicity of 0.52°. Data statistics are summarized in Table 1.

Auto-indexing using *HKL*-2000 clearly suggested a primitive orthorhombic space group. Systematic absences were observed along two of the three axes (reflection conditions: $h = 2n$, $k = 2n$). Thus, based on the diffraction pattern, we assigned space group $P2_12_12$ to this crystal form, which was proved to be correct by subsequent molecular replacement and refinement. The unit-cell parameters were a = 161.6, b = 87.4, c = 112.0 Å. Assuming the presence of four Cncat molecules in the asymmetric unit, the calculated Matthews coefficient ($V_{\rm M}$) was 2.5 Å^3 Da^{-1}, with a solvent content of 49.5%.

3.4. Molecular-replacement solution

The catalytic domain from the 2.1 Å resolution structure of auto-inhibited full-length human calcineurin (PDB entry 1aui) was used as the search model. Because of the flexibility of the terminal residues and the three mutations at the C-terminus, we excluded the N-terminal residues 20–26 and the C-terminal residues 341–347. We also omitted the dimetal (Zn^{2+}–Fe^{3+}) centre at the active site. As a result, we used a search model consisting of residues 27–340 from the A subunit with no water molecules for cross-rotation and translation searches.

Molecular replacement was straightforward in this case. The cross-rotation function gave a top four highest peaks which were 1.6 times higher than the mean peak value, suggesting that there are four molecules in the asymmetric unit, which is consistent with the $V_{\rm M}$ value. In the subsequent translation searches these top four cross-rotation solutions all gave the highest peaks, which were >2.6 times higher than the other peaks. The four solutions were combined to yield the initial model for the asymmetric unit.

We then performed the following to further confirm that the crystal belonged to space group $P2_12_12$ and that these four solutions are the correct molecular-replacement solutions. Firstly, visual inspection of the four-molecule initial model (Fig. 4*a*) in *O* (Jones *et al.*, 1991) revealed reasonable crystal packing with no molecular clashes. Secondly, subsequent rigid-body refinement using the initial model lowered the R factor and $R_{\rm free}$ to 33.5% and 33.0% from 42.3% and 43.0%, respectively, in the resolution range 20.0–2.87 Å (3.5% of all reflections were randomly selected as the $R_{\rm free}$ set). One round of simulated-annealing refinement further lowered the R factor and $R_{\rm free}$ to 30.5% and 30.8%, respectively. Finally, using this refined model, we calculated $\sigma_{\rm A}$-weighted $2F_{\rm o} - F_{\rm c}$ and $F_{\rm o} - F_{\rm c}$ maps, both of which clearly showed high densities at the active sites of all the four molecules for the characteristic dimetal (Zn^{2+}–Fe^{3+}) centre that was omitted in map calculation.

It is worthwhile pointing out that the Cn active site was found to be open to solvent channels in the crystal packing (Fig. 4*b*). Thus, this crystal form could permit complex formation by the ligand-soaking technique and may be a useful tool for the discovery of small-molecule inhibitors targeting the Cn active-site by crystallographic screening (Nienaber *et al.*, 2000) and for subsequent structure-based drug development.

In conclusion, we have crystallized a trypsin-resistant catalytic domain (residues 20–347 from the A subunit of human calcineurin α). We collected a diffraction data set to 2.87 Å resolution in space group $P2_12_12$ and obtained a clear molecular-replacement solution. The crystal structure of the active calcineurin catalytic domain will shed light on the activation mechanism of calcineurin by calmodulin. Moreover, this crystal form can be used for small-molecule inhibitor discovery by the crystal-soaking and/or cocrystallization methods.

This work was initiated when LJ was a postdoctoral fellow in Dr Stephen C. Harrison's laboratory at Harvard University. The authors thank Drs Anjana Rao, Patrick G. Hogan and José Aramburu for the calcineurin expression plasmid. The authors gratefully acknowledge the access to synchrotron radiation at National Synchrotron Light Source (beamline X25), Brookhaven National Laboratory.

References

Aramburu, J., Rao, A. & Klee, C. B. (2000). *Curr. Top. Cell. Regul.* **36**, 237–295.
Aramburu, J., Yaffe, M. B., López-Rodríguez, C., Cantley, L. C., Hogan, P. G. & Rao, A. (1999). *Science*, **285**, 2129–2133.
Baba, Y., Hirukawa, N. & Sodeoka, M. (2005). *Bioorg. Med. Chem.* **13**, 5164–5170.
Baba, Y., Hirukawa, N., Tanohira, N. & Sodeoka, M. (2003). *J. Am. Chem. Soc.* **125**, 9740–9749.
Bai, J. P. F., Lesko, L. J. & Burckart, G. J. (2010). *Pharmacotherapy*, **30**, 195–209.
Brünger, A. T., Adams, P. D., Clore, G. M., DeLano, W. L., Gros, P., Grosse-Kunstleve, R. W., Jiang, J.-S., Kuszewski, J., Nilges, M., Pannu, N. S., Read, R. J., Rice, L. M., Simonson, T. & Warren, G. L. (1998). *Acta Cryst.* D**54**, 905–921.
Clipstone, N. A. & Crabtree, G. R. (1992). *Nature (London)*, **357**, 695–697.
DeLano, W. L. (2002). *PyMOL*. http://www.pymol.org.
Griffith, J. P., Kim, J. L., Kim, E. E., Sintchak, M. D., Thomson, J. A., Fitzgibbon, M. J., Fleming, M. A., Caron, P. R., Hsiao, K. & Navia, M. A. (1995). *Cell*, **82**, 507–522.
Halloran, P. F. (2004). *N. Engl. J. Med.* **351**, 2715–2729.
Hoorn, E. J., Walsh, S. B., McCormick, J. A., Fürstenberg, A., Yang, C.-L., Roeschel, T., Paliege, A., Howie, A. J., Conley, J., Bachmann, S., Unwin, R. J. & Ellison, D. H. (2011). *Nature Med.* **17**, 1304–1309.
Huai, Q., Kim, H.-Y., Liu, Y., Zhao, Y., Mondragon, A., Liu, J. O. & Ke, H. (2002). *Proc. Natl Acad. Sci. USA*, **99**, 12037–12042.
Jin, L. & Harrison, S. C. (2002). *Proc. Natl Acad. Sci. USA*, **99**, 13522–13526.
Jones, T. A., Zou, J.-Y., Cowan, S. W. & Kjeldgaard, M. (1991). *Acta Cryst.* A**47**, 110–119.

Kissinger, C. R. *et al.* (1995). *Nature (London)*, **378**, 641–644.
Klee, C. B., Crouch, T. H. & Krinks, M. H. (1979). *Proc. Natl Acad. Sci. USA*, **76**, 6270–6273.
Li, H., Zhang, L., Rao, A., Harrison, S. C. & Hogan, P. G. (2007). *J. Mol. Biol.* **369**, 1296–1306.
Liu, J., Farmer, J. D., Lane, W. S., Friedman, J., Weissman, I. & Schreiber, S. L. (1991). *Cell*, **66**, 807–815.
Nienaber, V. L., Richardson, P. L., Klighofer, V., Bouska, J. J., Giranda, V. L. & Greer, J. (2000). *Nature Biotechnol.* **18**, 1105–1108.
O'Keefe, S. J., Tamura, J., Kincaid, R. L., Tocci, M. J. & O'Neill, E. A. (1992). *Nature (London)*, **357**, 692–694.
Otwinowski, Z. & Minor, W. (1997). *Methods Enzymol.* **276**, 307–326.
Roehrl, M. H., Kang, S., Aramburu, J., Wagner, G., Rao, A. & Hogan, P. G. (2004). *Proc. Natl Acad. Sci. USA*, **101**, 7554–7559.